Research Article

Received: 18 December 2020 Revised: 4 March 2021 Accepted article published: 5 March 2021 Published online in Wiley Online Library:

(wileyonlinelibrary.com) DOI 10.1002/jctb.6728

Pre-deposited dynamic membrane adsorber formed of microscale conventional iron oxide-based adsorbents to remove arsenic from water: application study and mathematical modeling

Muhammad Usman,[a*] Aida Idrissi Belkasmi,[a] Ioannis A Kastoyiannis[b] and Mathias Ernst[a]

Abstract

BACKGROUND: This study reports the development of a dynamic membrane (DM) adsorber by pre-depositing powdered-sized-fraction of iron oxide-based adsorptive material on the surface of a microfiltration(MF) membrane. The aim is to use the developed DM adsorber for arsenate (As(V)) remediation from water by a combined mechanism of adsorptive and membrane filtration. The two applied iron oxide-based adsorptive materials are micro-sized granular ferric hydroxide and micro-sized tetravalent manganese feroxyhyte, and are available at affordable price.

RESULTS: The results show that As(V) removal efficiency strongly depends on the physicochemical properties of the depositing material such as specific surface area, isoelectric point and particle size of the pre-depositing material. The experimentally determined As(V) removal rates were mathematically modeled using a homogeneous surface diffusion model, which incorporates the equilibrium parameters and mass transport coefficients of the adsorption process. The simulations showed that the mathematical model could describe the As(V) removal rates accurately over a broad range of operating conditions. The results further showed that the longer filtration times with very low normalized As(V) permeate concentration ($C/C_f = 0.1$, for example) can be prolonged by operating the DM adsorber at the lowermost membrane water flux of 31 L m^{-2} h^{-1} and a large amount of pre-depositing material on the MF membrane surface ($M_a = 14$ mg cm^{-2}).

CONCLUSION: The results presented in this study confirm that use of these inexpensive materials (side-product of granular iron oxide-based adsorbents) in treating As(V)-polluted water would enhance the sustainability of the industrial production process of conventional granular adsorbents by utilizing the wastes created during the process of adsorbent production.

Supporting information may be found in the online version of this article.

Keywords: arsenate; adsorption; granular ferric hydroxide; membrane adsorber; homogenous surface diffusion model; water treatment

INTRODUCTION

Dynamic membranes (DMs) were first narrated in 1965 by a research group from the Oak Ridge National Laboratory.[1] Unlike a membrane manufactured through a casting membrane solution or melting spinning technique, a DM filter, which is referred to as a 'secondary membrane', can be developed *in situ*. The DM filter builds up as a layer of particles such as metal oxides, soil-based compounds and powdered activated carbon (PAC) deposited via permeation drag onto surfaces of meshes, nylon, polyethersulfone (PES) and ceramic-based microfiltration (MF) and ultrafiltration (UF).[2–4] This suggests that a DM filter technology predominantly involves two layers, namely the primary membrane as a supporting layer and the deposited cake layer of microparticles as the secondary membrane. The primary membrane offers the foundation to the deposited layer, while the

* *Correspondence to: M Usman, Institute for Water Resources and Water Supply, Hamburg University of Technology, Am Schwarzenberg-Campus 3, 20173 Hamburg, Germany. E-mail: muhammad.usman@tuhh.de*

a *Institute for Water Resources and Water Supply, Hamburg University of Technology, Hamburg, Germany*

b *Laboratory of Chemical and Environmental Technology, Department of Chemistry, Aristotle University of Thessaloniki, Thessaloniki, Greece*

deposited layer, consisting of nano- and microparticles, acts as the dominant functional part for decontamination of water.[5] The deposited layer of particles then determines the removal rates and efficiency of the DM filter towards a target trace pollutant,[2,6] when the primary membrane does not have a rejection capacity towards the specific target pollutant.[2] For example, dissolved inorganic trace contaminants such as arsenic and antimony are not retained by a typical MF or UF membrane.[7] Modification of such a membrane, i.e. by iron oxides, can remove the trace contaminant by adsorption onto the secondary membrane, while the primary membrane achieves high overall water quality by filtering out suspended particles.[8]

The DM filter with diverse separating functions can be developed by opting suitable pre-depositing materials. The DM filter made on loosened support materials such as MF and mesh has an advantage over traditional membranes of operating under gravity-driven mode.[5] A driving force by means of a 10 cm water head was sufficient during DM filtration of secondary wastewater effluent to achieve 200 L m^{-2} h^{-1} when a nylon mesh with an corresponding aperture of 25 μm was applied as a DM support material.[9] Furthermore, once the DM filter is fouled or exhausted, the deposited cake layer can be displaced by backwashing either with water or air,[10] and a new cake layer of depositing material can be readily redeposited. The use of water has proved to be an effective cleaning approach for the exhausted DM filter. More than 90% of the primary membrane permeability could be restored after four filtration cycles.[11,12]

DM filters are categorized into two main types: self-forming DM filters and pre-deposited DM filters. In the first case, the feed constituents are those which form the DM filter, whereas the pre-deposited DM filter are developed as a result of deposition of particles other than the feed solution at the top surface of the primary membrane prior to the inflow of the polluted water.[2,4,5] The pre-deposited DM filter offers the flexibility of selecting appropriate and affordable materials which might be used to develop the membrane filter. Irrespective of DM filter category, the DM either: (a) expands the capability of the primary membrane to remove contaminants that otherwise would not be removed; (b) enhances the overall performance of the conventional primary membrane; or (c) conserves the primary membrane from fouling.[4]

According to the formation mechanism, DM filters can be classified into two classes. Class I DM filters are those whereby the pore size of the primary membrane is really small, to completely retain the DM filter-forming material. In this case, the dominant mechanism that governs DM formation is the concentration polarization.[13] When the primary membrane's pore diameter is significantly larger than the size of the particles (e.g. dust or bacteria) to be deposited, these types of DM filters are referred to as class II DM filters. The depositing materials can form a bridge-like structure over the pores and may build flocculation centers. The pore constriction and cake filtration are membrane-forming mechanisms that are involved in the formation of class II DM filters.[4] Generally, in DM filtration technology a cake layer of specific thickness is explicitly formed as more and more particles are deposited on the surface of the primary membrane. As a result, resistance might not be as badly affected during the formation of class I DM filters compared to class II DM filters.[4,13] Therefore, class I DM filters have recently gained popularity in water treatment for removal of organics.[14,15]

The most popular materials used in DM filtration technology are polymers, hydrous Zr(IV) oxide polymer, metal oxides, soil-based materials such as kaolin and diatomite, PAC and nanoparticles. Among these materials, PAC and oxides of iron, aluminum and titanium were the first to be applied, whereas nanoparticles are gaining popularity and are now widely accepted as DM-forming materials.[4] Iron oxide-based adsorbents (e.g. Fe_2O_3) have been used as pre-depositing material not only for fouling mitigation of the primary membrane in UF applications[12,16] but also for purification purposes.[16] A DM filter formed by pre-depositing PAC particles onto a primary membrane showed excellent efficiency in adsorbing organic pollutants from diluted textile wastewater.[17] Soil-based materials have also been tested as DM filter-forming materials, examples of which are clay in treating domestic wastewater,[18] clay for color removal[19] and arsenic removal[20] through adsorption.

On a global scale, arsenic is considered to be a main environmental issue because of its presence in the groundwater and surface water sources; this is of great relevance to environmentalists because of its toxicity and carcinogenicity, and the number of affected people worldwide.[21–23] It enters the food chain either through drinking water or by consuming arsenic-containing food, e.g. rice.[24] Arsenic in polluted environments primarily exists as arsenite and arsenate, abbreviated as As(III) and As(V), respectively. Arsenic naturally occurs in over 200 different mineral forms, of which approximately 60% are arsenates, 20% sulfides and sulfosalts and the remaining 20% include arsenides, arsenites, oxides, silicates and elemental arsenic.[25] As(V) anions prevail in oxygenated water, whereas As(III) anions occur in moderately reduced environments (e.g. anoxic groundwater). Under oxidizing conditions, $H_3AsO_4^-$ is the more stable species between pH 2 and 7, whereas $H_2AsO_4^{2-}$ is the more stable species above pH 7 in natural waters.[26,27] Several treatment technologies for arsenic removal from drinking water have been applied worldwide,[28] and the most commonly used are chemical coagulation using metal (iron) salts,[29–31] sorption on activated alumina,[32–34] iron oxides and iron oxyhydroxides,[35–40] electrocoagulation with Fe/Al electrodes,[41] preliminary arsenic oxidation by ozonation or biological oxidation,[42] ion exchange using polymer resins[43] and pressure-driven membrane processes, such as nanofiltration[44] and reverse osmosis.[45–47] Among the several existing arsenic removal technologies, chemical precipitation by ferric coagulation followed by filtration and adsorption onto iron oxides and iron oxyhydroxides appear to be cost effective for large-scale arsenic treatment plants to comply with established WHO guideline value of 10 μg L^{-1}.[35,40,48] Chemical precipitation by ferric coagulation has significantly higher arsenic removal efficiencies compared to iron-based adsorbent materials, including iron oxyhydroxides. However, the efforts required for handling the wastes from coagulation–filtration prevent its application when the treatable volume of product water corresponds to the one produced for a small town.[35,48] Adsorption technology using iron oxyhydroxides is considered to be an economical and effective technique for arsenic removal because of its lower cost and availability of suitable commercial adsorbents and their regeneration.[49,50] It is generally believed that arsenic adsorption by porous iron hydroxides takes place not only due to Coulombic and/or Lewis acid–base interactions but also because of formation of monodentate and bidentate inner-sphere complexes.[51,52] It is widely acknowledged that the porous character of iron (oxy)hydroxides adsorbs As(V) at internal iron complexation sites.[53]

In the present work, the main objective was to create a pre-deposited DM filter based on the utilization of micro-sized powdered fractions of iron oxide-based adsorbents, namely micro-

Journal of Chemical Technology and Biotechnology published by John Wiley & Sons Ltd on behalf of Society of Chemical Industry (SCI).

sized granular ferric hydroxide (μGFH) and micro-sized tetravalent manganese feroxyhyte (μTMF). μGFH comprises the by-products (waste) of the industrial production process of the commercially available granular GFH and which is currently discarded, whereas μTMF is generated during the production of TMF at the laboratory scale. Both adsorbent materials are excellent arsenic adsorbents and exhibit remarkable adsorption affinity towards As(V). A previous study of our group indicated that the adsorption capacities of μGFH at an equilibrium arsenic concentration of 10 μg L^{-1} and pH 8 were found to be 6.9 μg As(V) mg^{-1} and 3.5 μg As (III) mg^{-1}, respectively; whereas for μTMF the adsorption capacities were 5.5 μg As(V) mg^{-1} and 4.8 μg As(III) mg^{-1} under the same experimental conditions.[54] Further, a recent study of our group has shown that side-products of iron oxide-based adsorbents might be employed in an adsorption–MF hybrid system wherein the adsorption take place in a slurry reactor simulating a completely mixed stirred tank reactor. This study also concluded that the powdered-sized fractions of the studied adsorbents have an overwhelming influence on As(V) adsorption rate compared to larger-sized fractions (>63 μm).[8] Accordingly, the micro-sized powdered fractions of iron (oxy)hydroxides might be applied as pre-depositing materials for *in situ* preparation of DM filters. In the present study, we moved forward the research by applying the powdered-sized fractions of iron oxide-based adsorbents as DM filter-forming materials and a novel modeling approach to describe in more detail the efficiency of As(V) removal and the parameters that influence the effectiveness of the process. We applied a mass transfer model to describe As(V) removal in the permeate of the pre-deposited DM adsorber. Furthermore, this study aims at identifying the best operating conditions for optimum As(V) removal from groundwaters. Application of the modeling approach will support the optimization and facilitate the application of DM filtration technology in real arsenic treatment systems.

Until now, all reported pre-deposited DM filters were focused on factors affecting the formation and mechanisms by which the DM filters are formed. In the present work, we investigated for the first time the performance potential of two powdered-sized conventional iron hydroxides (μGFH and μTMF) as pre-depositing materials of DM filter to remove As(V) from water in the MF process and proposed a mathematical model to describe the overall performance of the presented process.

MATERIALS AND METHODS

Materials

In the present work, the pre-deposited layer of applied adsorbents on the primary MF membrane was made by powdered-sized fractions (1–63 μm) of GFH and TMF. The chosen pollutant was As(V), as iron-based adsorbents such as GFH and TMF are customarily applied to the treatment of arsenic-polluted waters in a natural environment. Flat sheet PES-based MF membranes (DURAPES200) with a nominal size of 0.2 μm used a primary membrane were purchased from Membrana GmbH (Wuppertal, Germany).

The industrial-scale production of μGFH (GEH Wasserchemie GmbH & Co., Osnabrück, Germany) involves the neutralization of an $FeCl_3$ solution and precipitation with NaOH. It mainly comprises of akagenéite mineral.[55] The lab-scale synthesis of μTMF includes co-precipitation of $FeSO_4$ and $KMnO_4$. It is identified as feroxyhyte.[56] The important physicochemical properties of the applied adsorbents were determined in our former studies[54,57] and are reported in Table 1. Table 1 lists the specific surface area which were estimated according to Brunauere-Emmette-Teller (BET) model and details on BET surface area measurements can be found in our previous work.[57]

A sieve having a mesh size of 63 μm was applied to separate powdered-sized μGFH (1–63 μm) from air-dried μGFH (1–250 μm). The same sieve was applied to acquire powdered-sized μTMF (1–63 μm) from μTMF (1–250 μm). The individual particle size of the majority (>98%) of μGFH (1–63 μm) particles was smaller than 5 μm, while 100% particles of μTMF (1–63 μm) were smaller than 5 μm. Consequently, the mean particle size of the powdered-sized μGFH and μTMF materials was 3.5 and 2.8 μm, respectively. The particle size distribution of powdered-sized μGFH and μTMF is provided in Supporting Information Figs S1 and S2).

Arsenic-polluted water was obtained by spiking an appropriate aliquot of As(V) standard solution (Merck Chemicals GmbH, Germany) in deionized (DI) water. A buffer (*N*,*N*-bis(2-hydroxyethyl)-2-aminoethanesulfonic acid (BES; 2 mmol L^{-1}) was carefully supplemented to prepare As(V)-polluted water (Carl Roth GmbH + Co. KG, Germany) to promote pH control for longer periods. Before continuous feeding tests, a target pH of 8 ± 0.1 was set by addition of either NaOH or HCl.

Experimental setup

Each dead-end DM filtration experiment was divided into three stages: preparation of primary MF membrane as a porous support material, pre-deposition of adsorbent particles (DM filter formation) and filtration experiments employing pre-deposited DM adsorber.

To prepare for the employment of the primary MF membrane as porous support material for the deposition of powdered-sized iron oxide-based adsorbents, the primary MF membrane was first rinsed with at least 1 L of pure water to remove residual substances. An Amicon® 8200 filtration cell constructed by Millipore (USA) was used for the formation of the pre-deposited MD filter as well as for the continuous dead-end filtration experiments. The top-end piece of filtration cell contains the feed inlet, while the bottom of the cell contains a porous insert that holds a membrane with an active surface of 28.7 cm^2.

A μGFH and μTMF pre-deposited DM adsorber was formed according to the following procedure: the suspension formed from mixing powdered-sized fractions of applied adsorbents (300 or 400 mg in 150 mL pure water) was transferred to a filtration cell housing the primary MF membrane. The cell was then sealed with an upper cap and O-ring. The pure water (~0.5 L) was filtered at 0.5 bar applied filtration pressure through each membrane and a new membrane was applied to all experiments. A uniform thin cake layer of adsorbent particles was formed at the surface of the primary MF membrane by permeation drag, which is the convective force dragging the particles towards the primary membrane.

Once the DM adsorber was formed by pre-depositing the powdered-sized fractions of applied adsorbents at the primary membrane surface, feed solution containing different concentration levels of As(V) (either 190 or 380 μg L^{-1}) at room temperature (20 ± 2 °C) was introduced using a peristaltic pump from a solution reservoir through the membrane filtration cell (Fig. 1). Experiments using constant flux filtration, which is mainly used in plant practice filtration, rather than constant pressure, were carried out by keeping the water flux constant while changes in the operating filtration pressure were continuously monitored. A signal-conditioned pressure gauge (Sensortechnics GmbH, Germany) collected the operating pressure data automatically. As(V)

Journal of Chemical Technology and Biotechnology published by John Wiley & Sons Ltd on behalf of Society of Chemical Industry (SCI).

Table 1. Physicochemical properties of applied iron oxide-based adsorbents[54, 57]

Material	Iron content (wt%)	Mean particle diameter (μm)	Moisture content (%)	BET surface area ($m^2\ g^{-1}$)	Pore volume ($mL\ g^{-1}$)	Pore diameter (nm)	Isoelectric point	Particle density ($g\ cm^{-3}$)
μGFH	60	3.5	~50	283 ± 3	0.28	2.6	7.8 ± 0.2	1.550
μTMF	44	2.8	<5	178 ± 8	0.35	3.2	7.2 ± 0.1	0.642

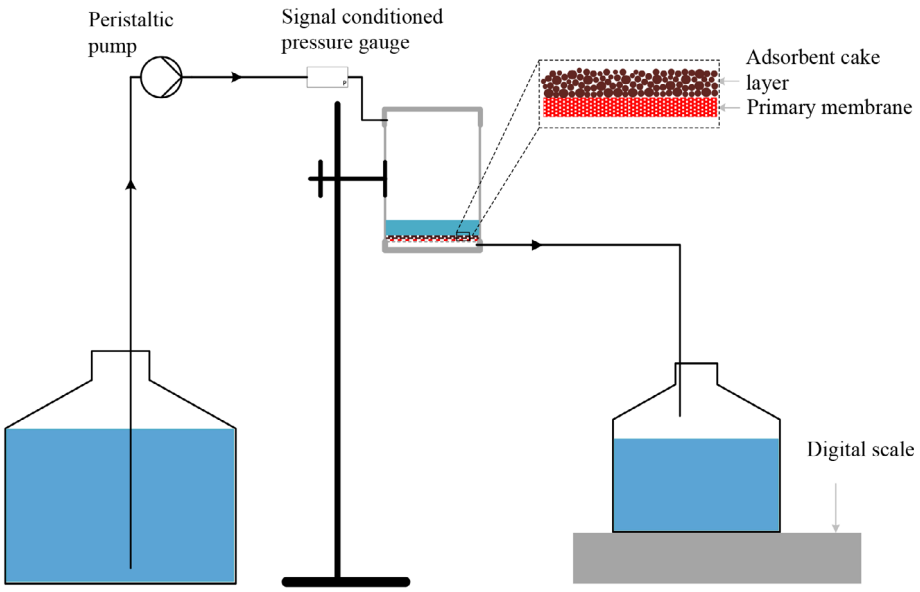

Figure 1. Schematic representation of the laboratory installations for dead-end filtration. Inset demonstrates the pre-deposited cake layer of applied iron oxide-based adsorbent material.

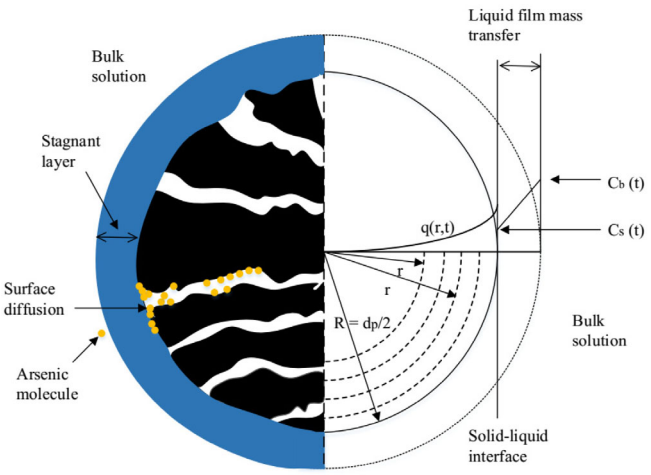

Figure 2. Schematic diagram of arsenic ion mass transport from the bulk solution into a particle of porous iron oxide.

concentration levels in the effluent of a pre-deposited DM adsorber were monitored by collecting samples at different time intervals. The performance pre-deposited DM adsorber was evaluated under different operating conditions. The recorded As(V) removal rates were then modeled using a mathematical model based on a mass transfer model called the 'homogeneous surface diffusion model (HSDM).

Arsenic analysis

Collected permeate samples were measured for total arsenic at pH 2 using HCl. Measurement of arsenic concentration in the feed and permeate samples was carried out by graphite furnace atomic absorption spectrophotometry (GFAAS; 4110 ZL instrument, PerkinElmer, Germany). GFAAS was operated with a graphite furnace tube atomizer. The arsenic samples were atomized using argon gas. GFAAS was set up with a lamp current of 380 mA, wavelength 193.7 nm for arsenic detection, and a slit width of 0.7 nm. The peak area was selected as a measurement mode. The arsenic limit of detection of this method was 0.5 μg L^{-1}. The maximum standard deviation of the analysis was 5%.

Mathematical modeling of permeate As(V) concentration

A mathematical model incorporating the HSDM has been applied to describe the concentration profiles of arsenic adsorption systems,[8,58–61] These studies have demonstrated that the HSDM allows the simulation of the dynamic behavior of a variety of adsorbates (phosphate, arsenic, chloroform and vanadium) onto porous adsorbents (e.g. activated carbon, GFH and μGFH), as long as the mass transfer from the solution to the adsorption sites within the adsorbent particles is constrained by mass transfer resistances such as surface diffusion and external film mass transfer, as depicted in Fig. 2.

The HSDM model assumes that the adsorbate (e.g. As(V)) diffuses through a stagnant liquid film layer developed around an adsorbent particle into a homogeneous adsorbent sphere. The

Journal of Chemical Technology and Biotechnology published by John Wiley & Sons Ltd on behalf of Society of Chemical Industry (SCI).

surface diffusion and the external film diffusion are the mass transfer resistances incorporated into the HSDM controlling arsenic adsorption.[62] The mass transfer resistance arises from surface diffusion (D_s) and the external film diffusion (k_f).

The HSDM is an adsorption model that comprises two partial differential equations. Equation (1) (referred to as the filter mass balance equation) describes the mass transport through the adsorbent layer, whereas the mass transfer into the adsorbent particle is represented by Eqn (2) (intra-particle mass transfer equation). The assumptions made in the HSDM are: (i) plug–flow conditions in the deposited cake layer; (ii) the adsorbent particles are spherical; (iii) local adsorption equilibrium occurs within the adsorbent particle; (iv) instantaneous adsorption takes place on active adsorption sites; (v) intra-particle surface diffusion is predominately mass transfer resistance; (vi) solid-phase mass transfer owing to surface diffusion remains constant for an adsorbent. A detailed description of the model has been reported elsewhere.[58]

The As(V) mass balance over the pre-deposited DM filter in linear coordinates (z) is

$$\varepsilon_B \frac{\partial C}{\partial t} + v_f \frac{\partial C}{\partial z} - \frac{3(1-\varepsilon_B)}{R} k_f (C - C_s) = 0 \quad (1)$$

here t is time, v_f is filter velocity, $\varepsilon_B$is cake layer porosity, R is particle radius, k_f is mass transfer coefficient due to the external film diffusion, and C and C_s are adsorbate liquid-phase concentration in the pre-deposited iron oxyhydroxides layer and at the solid–liquid interface, respectively.

The intra-particle mass transfer equation indicates adsorbate transfer in the adsorbent particle in radial coordinates (r) in proportion to Fick's second law of diffusion:

$$\frac{\partial q(r,t)}{\partial t} = D_s \left[\frac{\partial^2 q(r,t)}{\partial r^2} + \frac{2\partial q(r,t)}{r\,\partial r} \right] \quad (2)$$

where q is adsorbate solid-phase concentration and D_s is mass transfer caused by surface diffusion. The initial condition and boundary conditions of the Eqn (2) can be found in the Supporting Information.

For model solution, desktop software (FAST 2.1) developed by Sperlich *et al.*[58] was applied. The parameters to solve Eqns (1) and (2) include readily measurable mass- and volume-related parameters, i.e. mass of adsorbent applied, mean particle diameter, particle density, cake layer density, influent adsorbate concentration) and indirectly quantifiable parameters such as adsorption equilibrium and kinetic parameters. It has been proven that the mathematical model based on the HSDM has the capacity to describe the impact of water chemistry (e.g. pH and water matrix) on adsorbate dynamic behavior if the adsorption equilibrium and kinetic parameters under changed water quality conditions are available (have been derived).[60,61] This software (FAST 2.1) provides a numerical solution of Eqns (1) and (2) to simulate the concentration profile of anions over time of a fixed-bed adsorption filter packed with an adsorbent used in water treatment.

RESULTS AND DISCUSSION

Pre-deposited DM adsorber for As(V) removal

Figure 3 shows the normalized As(V) concentration with respect to feed As(V) concentration in the permeate of primary MF membrane and pre-deposited DM adsorber as a function of the specific throughput volume, expressed as volume of treated water per unit area of primary membrane, for the two applied adsorbents applied as DM filter-forming materials at pH 8 ± 0.1.

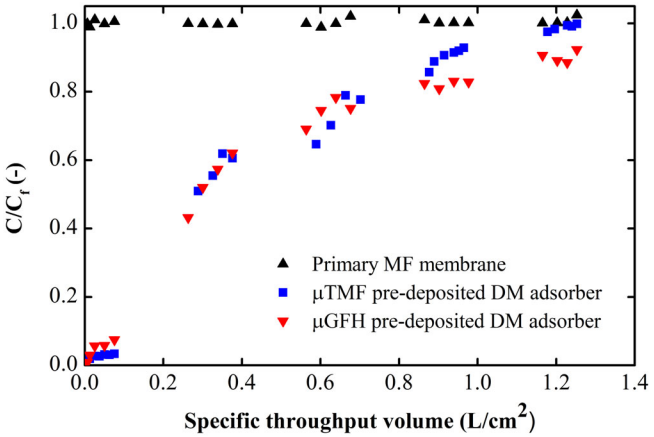

Figure 3. Normalized permeate concentrations of As(V) as a function of specific throughput volume by primary MF membrane and pre-deposited DM adsorber formed of μGFH and μTMF at 125 L m^{-2} h^{-1}, amount of adsorbent at 10.4 mg cm^{-2}, feed As(V) concentration = 380 μg L^{-1} and pH 8.

The results demonstrate that the primary MF membrane did not lead to a reduction in normalized As(V) permeate concentration (Fig. 3) because the nominal pore size of the primary MF membrane is 0.2 nm, which is one order of magnitude larger than the dominant As(V) species at pH 8 (ionic radius of $HAsO^{2-}$ is 0.397 nm[63]). Additionally, the PES-based membrane is negatively charged at pH 8,[64] and consequently the As(V) removal by electrostatic attractive forces is not imaginable. On the other hand, at constant water flux of 125 L m^{-2} h^{-1} and adsorbent dosage (M_a), expressed as amount of As(V) adsorptive material pre-deposited per unit area of primary MF membrane, of 10.4 mg cm^{-2}, the pre-deposited DM adsorber results in an immediate decrease in normalized As(V) permeate concentration, with the As(V) concentration reaching a minimum value. The DM adsorber achieved very high As(V) removal efficiency (90%, which corresponds to $C/C_f = 0.1$) for the first 0.15 L cm^{-2} specific throughput volume. Subsequently, the normalized As(V) permeate concentration started to increase as the volume of treated water was increasing further (Fig. 3). This was due to the saturation of the deposited adsorbent layer caused by the continuous inflow of As(V)-contaminated feed solution. In the case of μTMF pre-deposited DM adsorber, the rise in normalized As(V) permeate concentration was slower than when using the μGFH deposited layer, even though the achieved As(V) adsorption capacity of μTMF (15.4 μg mg^{-1}) was lower than that achieved by using the μGFH (22.4 μg mg^{-1}) at 380 μg L^{-1} and at pH 8.[8] This is most likely due to the smaller particle size of μTMF, even though the BET surface area and isoelectric point of μTMF is lower than μGFH (Table 1). The second explanation might be the large pore diameter of μTMF, which is causing a more rapid As(V) diffusion inside the adsorptive material. A similar trend of As(V) removal rates by μTMF and μGFH was observed during As(V) batch adsorption tests carried out in the slurry reactor setup.[8] As the volume of treated water increased, the normalized As(V) permeate concentration started to increase. Interestingly, an increase in normalized As(V) concentration was rapid in the case of the μTMF pre-deposited layer after 0.8 L cm^{-2} specific throughput volume (Fig. 3). This can be ascribed to the fact that the adsorption process is restricted to

Journal of Chemical Technology and Biotechnology published by John Wiley & Sons Ltd on behalf of Society of Chemical Industry (SCI).

the number of available active sites on the adsorbent surface. As the process continues, the more active sites are more rapidly consumed in the case of μTMF as compared to μGFH and thus, at the final stage of the process, remaining active sites of μTMF were consumed by As(V) at a faster rate than μGFH. Moreover, the adsorption capacity of μTMF is smaller than μGFH, due to which recorded normalized concentration of As(V) ≈ 1 has occurred at the end of the experiment (~0.9 in the case of μGFH) when specific throughput volume was 1.25 L cm^{-2}. Moreover, the reproducibility of the pre-deposited DMs was also tested in order to increase the acceptability of these filters in water treatment, and the As(V) removal rates for the two developed DM adsorbers were nearly identical under the same operating conditions (Supporting Information Fig. S4).

The presented results indicate that the lifetime of the pre-deposited DM adsorber largely depends on the type of pre-depositing material, micro-pores and particle size of the deposited material as well as on the specific surface area, which determines the number of active energy sites and the accessibility of the pollutant to the adsorbent material.[65]

Mathematical modeling of As(V) removal rates in a dynamic membrane adsorber

The Freundlich constants (K_F and n) and D_s values are based on our previous batch adsorption experiments.[8] Freundlich parameters were derived from batch adsorption equilibrium, whereas D_s values were determined by fitting the kinetic data derived from batch adsorption kinetic experiments in the slurry reactor setup with model solution. The values of Freundlich parameters for μGFH adsorption are K_F = 4.5 μg mg^{-1} and n = 0.268. In the case of μTMF adsorption, the values of K_F and n are 3.5 μg mg^{-1} and n = 0.249, respectively. At an applied As(V) concentration 380 μg L^{-1} and pH 8, adsorption loadings determined through batch isotherm equilibrium tests in deionized water were found to be 22.4 and 15.4 μg mg^{-1} for μGFH and μTMF, respectively.[8] The values of adsorption equilibrium parameters and D_s are used as inputs to mathematically model As(V) removal rates.

The optimum k_f values are evaluated through a constant optimization procedure until the sum of square of error (SSE, Eqn (3)) is minimized. The SSE reflects the bias between the experimental and the simulated results. An SSE value close to zero describes the low bias, whereas larger values indicate relatively higher bias between the experimental data and model output:

$$\text{Sum of square of error} = \sum_{i=1}^{m} \left(\frac{C_{\text{model}}(i) - C_{\text{experiment}}(i)}{C_f} \right)^2 \quad (3)$$

Figure 4 shows permeate As(V) concentration profiles along with the model predictions expressed as C/C_f over the filtration time. This figure shows the model fit to the experimental data, which is considered to be satisfactory, evidenced from the high correlation (R^2) values and SSE values <1 (Table 2).

The measured model parameters at varying operating conditions are provided in Table 2. Using the D_s values determined at an As(V) concentration of 380 μg L^{-1} and the same pH in deionized water, it is evident that the model can accurately predict the As(V) removal rates at varying amounts of adsorbent material pre-deposited per unit area of primary membrane and membrane fluxes, which determine the contact time between the adsorbent pre-deposited layer and feed water. This is most likely due to the same concentration of As(V) applied in batch and continuous mode experiments. However, at a lower feed As(V) concentration of 190 μg L^{-1}, the model simulations slightly over-predict the As

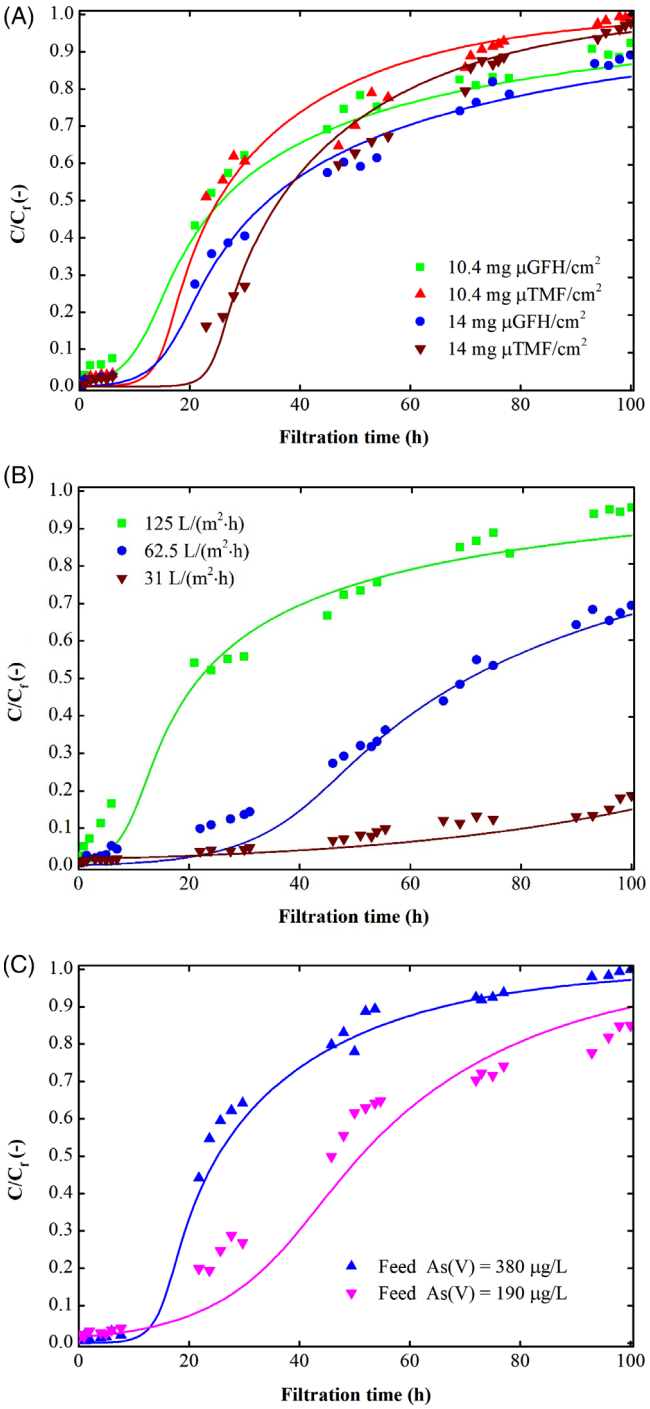

Figure 4. Experiments *versus* model prediction of As(V) removal rates representing influence of (A) amount of μTMF and μGFH pre-deposited per unit area of primary membrane at water flux = 125 L m^{-2} h^{-1}, feed As(V) concentration = 380 μg L^{-1} and pH = 8; (B) membrane water flux for μGFH pre-deposited DM adsorber at adsorbent dose (M_a) = 10.4 mg cm^{-2}, feed As(V) concentration = 380 μg L^{-1} and pH = 8; (C) feed As(V) concentration onto μTMF pre-deposited DM adsorber at adsorbent dose (M_a) = 10.4 mg cm^{-2}, water flux = 125 L m^{-2} h^{-1} and pH 8. Solid symbols reflect experimental data points, whereas model predictions are represented by solid lines under corresponding operating conditions.

Journal of Chemical Technology and Biotechnology published by John Wiley & Sons Ltd on behalf of Society of Chemical Industry (SCI).

Table 2. Measured model parameters under varying operational conditions

Material	Water flux (L m^{-2} h^{-1})	M_a (mg cm^{-2})	C_f (μg L^{-1})	Volume of water treated (L)	Final As(V) concentration C/C_f (–)	D_s(× 10^{-18} m^2 s^{-1})	k_f(× 10^{-6} m s^{-1})	R^2	SSE
μGFH	31	10.4	380	9	0.15	1.09	0.3	0.963	0.016
	62.5	10.4	380	18	0.67	1.09	1.0	0.995	0.042
	125	10.4	380	36	0.87	1.09	1.7	0.998	0.031
	125	14.0	380	36	0.83	1.09	1.6	0.993	0.027
	125	10.4	190	36	0.77	1.09	1.0	0.977	0.142
μTMF	31	10.4	380	9	0.21	2.26	0.07	0.980	0.019
	62.5	10.4	380	18	0.85	2.26	0.2	0.995	0.046
	125	10.4	380	36	0.98	2.26	1.0	0.998	0.029
	125	14.0	380	36	0.95	2.26	1.0	0.994	0.054
	125	10.4	190	36	0.90	2.26	0.3	0.974	0.169

M_a is the amount of pre-deposited adsorbent material per unit area of the primary membrane.

(V) removal rates, as evidenced by low correlation coefficient (R^2) and high SSE values.

The fitted k_f values decreased significantly with decreasing membrane flux for both adsorbent materials. Since the filter velocity has a direct influence on the boundary layer thickness, the film diffusion rate was reduced with decreasing membrane flux. Moreover, the k_f values were found to be higher for μGFH than μTMF under the same operating conditions. Large fitted k_f values for μGFH might be due to its higher adsorption loading towards As(V) than μTMF. These findings are consistent with previous studies,[59] in which larger k_f values for adsorbents were achieved with higher adsorbent capacity, during adsorption of nitrate onto commercially available and laboratory-prepared anion exchange resins in an adsorption–membrane hybrid process. A higher mass transfer at the external surface of the material provides a higher degree of adsorption for the target pollutant.

For the lower feed As(V) concentration of 190 μg L^{-1}, data in Table 2 show that the SSE value was 0.142 for μGFH and 0.169 for μTMF, demonstrating that the mathematical model is fairly consistent with the experimental data but unable to describe accurately the experimentally determined As(V) removal rates. The possible reason for higher SSE values between experimental and model results at different feed As(V) concentrations could be that the D_s value applied in the modeling approach was determined at the higher As(V) concentration of 380 μg L^{-1} in batch mode experiments. When optimum values of D_s and k_f are applied in the modeling approach, a strong agreement was observed, as indicated by improved goodness-of-fit parameters (R^2 = 0. 99 and SSE = 0.043 for μGFH pre-deposited DM adsorber and R^2 = 0.996 and SSE = 0.028 for μTMF pre-deposited DM adsorber). Several model simulations are shown in Fig. 5 employing values of D_s up to an order of magnitude lower. As can be clearly seen, model simulations captured the experimental data points much better when the fitted values of D_s were decreased from 2.26×10^{-18} to 1×10^{-18} m^2 s^{-1} and from 1.09×10^{-18} to 0.9×10^{-18} m^2 s^{-1} for μTMF and μGFH, respectively. The variation in D_s values might be due to dependence on the surface loadings. D_s dependence may exist for energetically heterogeneous adsorbents such as μGFH and μTMF, and could be explicated by the reduced adsorption energy with increasing surface loading that results in increased adsorbate mobility.[66]

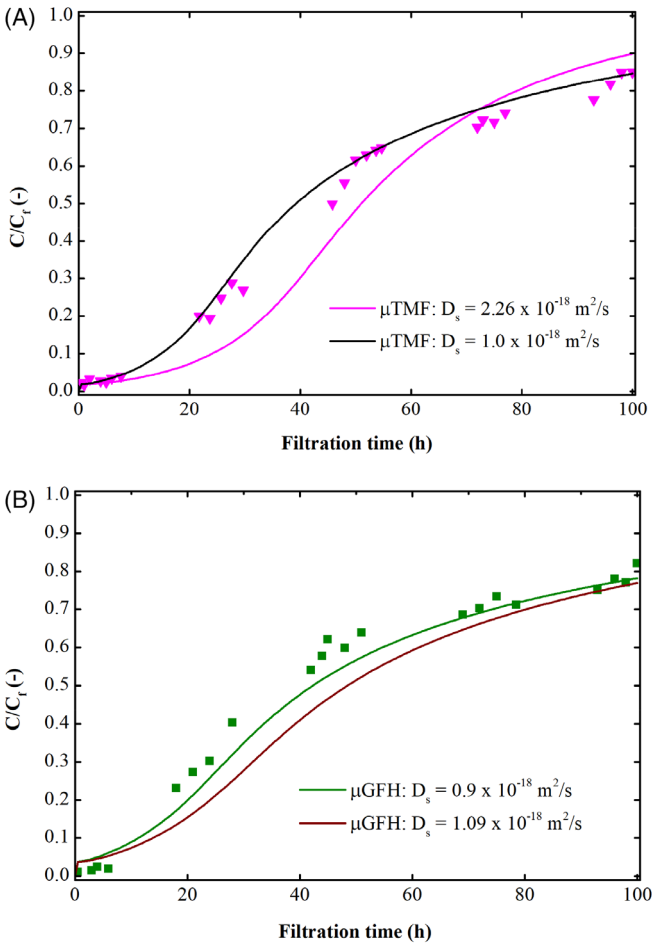

Figure 5. Model simulations of normalized As(V) concentrations employing different values of D_s for (A) μTMF pre-deposited DM adsorber; (B) μGFH pre-deposited DM adsorber at adsorbent dose (M_a) = 10.4 mg cm^{-2}, water flux = 125 L m^{-2} h^{-1} and pH 8.

In summary, the presented results indicate that a pre-deposited DM adsorber can be developed by pre-deposition of variable amounts of the powdered-sized fractions of applied adsorbents

Journal of Chemical Technology and Biotechnology published by John Wiley & Sons Ltd on behalf of Society of Chemical Industry (SCI).

on the primary membrane surface, which reveals that it is possible to regulate the thickness of the DM filter to treat the arsenic-polluted waters and achieve an As(V) removal efficiency of >90%, which corresponds to $C/C_f = 0.1$, as long as the best operating conditions such as lowermost membrane flux of 31 L m^2 h^{-1} and higher amount of pre-deposited adsorbent per unit area of primary membrane (14 mg cm^{-2}) were provided. Further, a higher flux governing shorter contact time has significantly improved the As(V) flux through the stagnant boundary layer surrounding an adsorbent particle, as indicated by large k_f values. A respective increase of one and two orders of magnitude for μGFH and μTMF pre-deposited DM adsorber was computed when membrane flux was increased from 31 to 125 L m^2 h^{-1}. Hence it can be concluded that k_f is related directly to the membrane water flux (contact time). Conversely, the surface diffusion coefficient (D_s) value is unique and not a function of membrane water flux and amount of adsorbent applied for DM filter formation, but is a function of feed As(V) concentration. We therefore propose investigating the effect of As(V) concentration on the D_s values to derive the relationship between As(V) concentration and D_s values to increase the acceptability of the applied mathematical model in the real water treatment system.

In this work, the size of individual adsorbent particle-forming DM adsorbers are significantly larger (one order of magnitude) than the primary membrane pores. Therefore, the pore size of the primary membrane is not anticipated to have a substantial influence on formation of the pre-deposited DM filter. However, more investigations are proposed to study the effect of the depositing particles on the surface morphology and strength of the primary membrane. These investigations would provide more insights into the repeating use of the primary membrane for formation and deformation of the DM filter.

Operating pressure

Long-term variations in operating pressure were monitored using a signal-conditioned pressure gauge. A stable operating pressure was recorded for 100 h constant flux dead-end flow experiments (data not shown here). This was possibly due to filtration of organic-free feed water. The operating pressure was in the range of 6–18 mbar for μTMF pre-deposited DM adsorber at $M_a = 10.4$ mg cm^{-2}, while for μGFH pre-deposited DM adsorber the range of operating pressure was 4–10.5 mbar (Figure 6). The operating pressure was higher for the higher water flux. This trend was attributed to the compression of deposited adsorbent cake layer on the membrane surface at higher membrane flux.[67] This trend was almost linear to the permeate water flux. At a higher M_a of 14 mg cm^{-2}, the operating pressure was 20 and 12 mbar for μTMF and μGFH pre-deposited DM adsorber, respectively. This is explained by a large volume of deposited cake layer on the surface of the primary MF membrane, which offers greater resistance to water flowing through the cake layer.

The operating pressures recorded for μGFH pre-deposited DM adsorber at all water fluxes were low when compared to μGFH pre-deposited DM adsorber possibly due to a lower volume of adsorbent cake layer (0.2 mL μGFH *vs*. 0.7 mL μTMF at $M_a = 10.4$ mg cm^{-2}).

Performance comparison of pre-deposited DM adsorber

The adsorption capacity of the powdered-sized adsorbents applied as pre-depositing materials for the formation of DM adsorber was calculated by integrating the breakthrough curve until $C/C_f = 1$ (referred to as $Q_{1.0}$) at a water flux of 125 L m^{-2} h^{-1} and adsorbent dosage of 10.4 mg cm^{-2}. The calculated $Q_{1.0}$ value of μGFH recorded through continuous-flow pre-deposited DM adsorber is 22.8 μg As(V) mg^{-1}, while the $Q_{1.0}$ value of μTMF is 15.8 μg As(V) mg^{-1}. Similar $Q_{1.0}$ values of μGFH and μTMF for As(V) were calculated when As(V) adsorption onto powdered-sized μGFH and μTMF in a slurry reactor was combined with MF at the same pH 8 (Fig. 7).[8]

In our previous study, the As(V) adsorption capacities of powdered-sized μGFH and μTMF were estimated to be 22.4 μg As (V) mg^{-1} and 15.4 μg As(V) mg^{-1}, respectively, which were determined through batch adsorption equilibrium experiments at a residual concentration of 380 μg L^{-1} and at pH 8. It can be concluded that adsorption capacities of powdered-sized μGFH and μTMF are the same when applied in three different experimental setups (Fig. 7).

For the applied iron oxide-based adsorptive materials, the As(V) adsorption capacities and bed volume treated (equivalent to a volume of water treated) the different water fluxes studied and

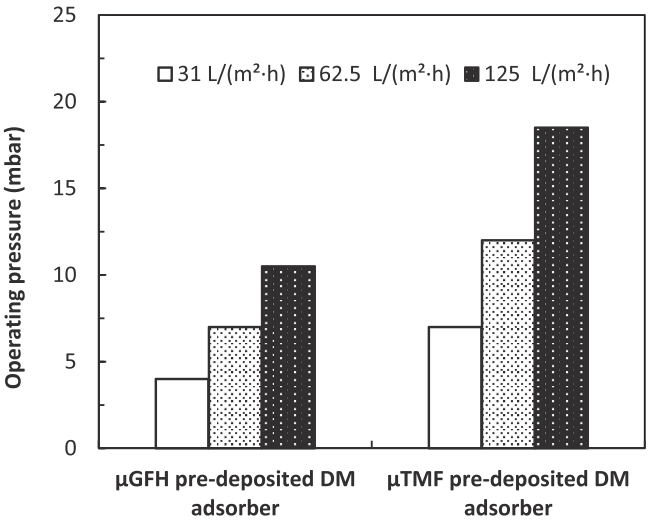

Figure 6. Operating pressure for the μGFH and μTMF pre-deposited DM filter at $M_a = 10.4$ mg cm^{-2}.

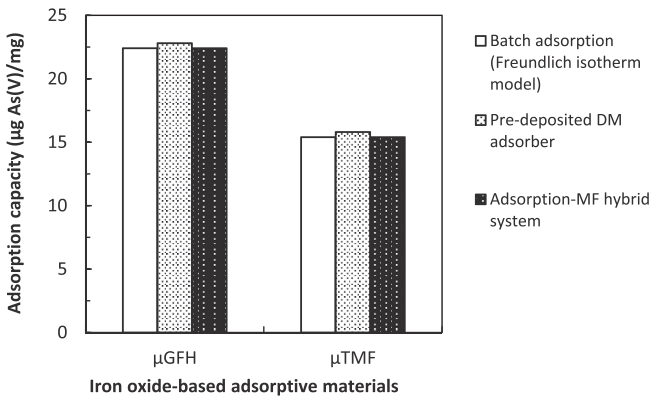

Figure 7. As(V) adsorption capacities achieved through pre-deposited DM adsorber compared to the adsorption capacities by the Freundlich isotherm model (obtained through batch adsorption experiments) and adsorption of As(V) onto micro-sized iron oxide-based adsorbents (μGFH and μTMF) in the slurry reactor of adsorption–MF hybrid system at $C_0 = 380$ μg L^{-1} and pH 8.

Journal of Chemical Technology and Biotechnology published by John Wiley & Sons Ltd on behalf of Society of Chemical Industry (SCI).

Table 3. Comparison of adsorption capacities of some adsorbents for As(V) reported in the literature with the adsorption capacities evaluated in this work (pH is shown in parentheses where reported)

Material	Type of experiment	Operating conditions	Bed volumes treated at $C/C_{in} = 0.1$	Adsorption capacity ($\mu g\ mg^{-1}$) at $C/C_{in} = 0.1$	Reference
GFH	Lab-scale column adsorber	Arizona groundwater As(V) = 100 $\mu g\ L^{-1}$, pH = 8.6, Mass of GFH = 2.78 g	3 000 at EBCT = 0.5 min 8 000 at EBCT = 2.5 min 11 000 at EBCT = 4.0 min	0.50 1.45 2.01	Westerhoff *et al.*[68]
Granular TiO_2	Lab-scale column adsorber	Groundwater As(V) = 400 $\mu g\ L^{-1}$, pH = 8.2, EBCT = 1.1 min	1 500	—	Cui *et al.*[69]
Bayoxide (E33)	Lab-scale column adsorber	Thessaloniki groundwater As(V) = 100 $\mu g\ L^{-1}$ pH = 7.3, EBCT = 1.2 min, mass of bayoxide = 8 g	— — —	3.09	Tresintsi *et al.*[35]
μTMF	Pre-deposited DM adsorber	Synthetic water As(V) = 380 $\mu g\ L^{-1}$, pH = 8.0, $M_a = 10.4\ mg\ cm^{-2}$	7 560 at 125 L $m^{-2}\ h^{-1}$ (EBCT = 7 s) 9 050 at 62.5 L $m^{-2}\ h^{-1}$ (EBCT = 14 s) 9 900 at 31 L $m^{-2}\ h^{-1}$ (EBCT = 28 s)	6.66 7.88 8.30	This work
μTMF	Pre-deposited DM adsorber	Synthetic water As(V) = 380 $\mu g\ L^{-1}$, pH = 8.0, $M_a = 14\ mg\ cm^{-2}$	9 450 at125 L $m^{-2}\ h^{-1}$ (EBCT = 7 s)	8.12	This work
μGFH	Pre-deposited DM adsorber	Synthetic water As(V) = 380 $\mu g\ L^{-1}$, pH = 8.0, $M_a = 10.4\ mg\ cm^{-2}$	14 400 at 125 L $m^{-2}\ h^{-1}$ (EBCT = 2 s) 21 600 at 62.5 L $m^{-2}\ h^{-1}$ (EBCT = 4 s) 36 450 at 31 L $m^{-2}\ h^{-1}$ (EBCT = 8 s)	3.55 5.32 8.77	This work
μGF	Pre-deposited DM adsorber	Synthetic water As(V) = 380 $\mu g\ L^{-1}$, pH = 8.0, $M_a = 14\ mg\ cm^{-2}$	22 320 at 125 L $m^{-2}\ h^{-1}$ (EBCT = 2 s)	5.19	This work

ECBT is the empty-bed contact time and expressed as adsorbent bed volume to the flow rate.
M_a is the adsorbent dose, expressed as amount of adsorptive material deposited per unit area of the primary MF membrane.

amount adsorbed applied to develop a DM adsorber are summarized in Table 3. The results demonstrate increasing As(V) adsorption capacities and bed volumes treated at decreasing water flux, which is explained by increasing contact time between adsorbent cake layer and As(V) species. Similarly, improved As(V) adsorption capacities were estimated at larger adsorbent dosages, which is attributed to a large number of available adsorption sites at higher $M_a = 14\ mg\ cm^{-2}$ relative to $M_a = 10.4\ mg\ cm^{-2}$. These observations lead to the conclusion that implementing lowermost water flux (31 L $m^{-2}\ h^{-1}$) and large amounts of adsorptive materials ($M_a = 14\ mg\ cm^{-2}$) to form pre-deposited DM adsorber are beneficial in treating As(V)-contaminated waters.

The adsorption capacities of powdered-sized μGFH and μTMF acquired through a pre-deposited DM filter can be compared with similar studies employing highly efficient commercial adsorbents for As(V) removal from water.[35,57,68,69] Although these studies have been executed under different experimental conditions (e.g. water matrix, influent As(V) concentration, pH and experimental setup), so the results of these studies cannot be directly compared. However, when the As(V) adsorption capacities and bed volumes treated are compared (Table 3), the studied powdered-sized iron oxide-based adsorptive materials are superior in remediating As(V) contaminated water even at very little contact time (7 and 2 s for μTMF and μGFH, respectively, because of extremely fast As(V) adsorption kinetics.[8]

CONCLUSIONS

In this study, a pre-deposited DM adsorber was developed *in situ* at low pressure (0.5 bar) by depositing the powdered-sized fractions of iron oxide-based adsorbents on the primary MF membrane, wherein the adsorbent deposited layer has acted as an adsorptive filtration barrier to remove As(V) from water applied in the MF process under varying operating conditions. Experimentally determined As(V) removal rates were described by a mathematical model incorporating surface diffusion and external film diffusion. The main findings are as follows:

(1) Applied adsorbents with individual particle size in the range of 2–3 μm were pre-deposited on the primary MF membrane to form a DM adsorber. The developed pre-deposited DM

Journal of Chemical Technology and Biotechnology published by John Wiley & Sons Ltd on behalf of Society of Chemical Industry (SCI).

adsorber shows remarkable As(V) removal efficiencies (as high as ~99%) with excellent reproducibility.

(2) μGFH and μTMF proved to be promising as emerging pre-depositing material for a DM filter and equally good for application in water treatment systems targeting As(V) removal.

(3) Parametric study indicates that As(V) removal rates of pre-deposited DM adsorbers can be controlled by changing the membrane water flux and amount of pre-depositing material per unit area of the primary membrane. Longer times of 90% As(V) removal can be achieved by increasing pre-depositing material over the primary membrane and lowering membrane water flux.

(4) As(V) removal rates of a pre-deposited DM adsorber can be accurately predicted using the applied mathematical model relying on the HSDM.

(5) The surface diffusion parameter of the HSDM can be considered as independent of membrane water flux and the amount of applied adsorbents used to form pre-deposited DM adsorber.

(6) Under the same operating conditions, the magnitude of the mass transfer due to external film diffusion was affected by the type of adsorbent material having different As(V) adsorption capacities. The k_f value was linearly related to the adsorption capacity of applied adsorbent material towards As(V).

(7) Low-pressure DM filtration technology is a sustainable and practicable approach that can be applied to remediation of arsenic-contaminated waters. The DM filtration technology may be further extended with repeated use of the exhausted iron oxide-based adsorbent materials to reduce the quantity of produced waste for environmental sustainability and to obtain more information on practical applications.

ACKNOWLEDGEMENTS

The authors are obliged to the German Academic Exchange Service (DAAD) for the fellowship of Mr Usman and the Hamburg University of Technology for resources. Professor Mitrakas, Department of Chemical Engineering, Aristotle University of Thessaloniki, Greece, and GEH Wasserchemie GmbH & Co., Osnabrück, Germany, are thanked for offering tetravalent manganese feroxyhyte and the micro-sized granular ferric hydroxide materials for the purposes of research. Open access funding enabled and organized by Projekt DEAL.

CONFLICTS OF INTEREST

The authors declare no conflict of interest.

SUPPORTING INFORMATION

Supporting information may be found in the online version of this article.

REFERENCES

1 Marcinkowsky AE, Kraus KA, Phillips HO, Johnson JS and Shor AJ, Hyperfiltration studies. IV. Salt rejection by dynamically formed hydrous oxide membranes. *J Am Chem Soc* **88**:5744–5746 (1966).
2 Ersahin ME, Ozgun H, Dereli RK, Ozturk I, Roest K and van Lier JB, A review on dynamic membrane filtration: materials, applications and future perspectives. *Bioresour Technol* **122**:196–206 (2012).
3 Matsuyama H, Shimomura T and Teramoto M, Formation and characteristics of dynamic membrane for ultrafiltration of protein in binary protein system. *J Membr Sci* **92**:107–115 (1994).
4 Anantharaman A, Chun Y, Hua T, Chew JW and Wang R, Pre-deposited dynamic membrane filtration: a review. *Water Res* **173**:115558 (2020).
5 Li L, Xu G and Yu H, Dynamic membrane filtration: formation, filtration, cleaning, and applications. *Chem Eng Technol* **41**:7–18 (2018).
6 Zhang X, Wang Z, Wu Z, Lu F, Tong J and Zang L, Formation of dynamic membrane in an anaerobic membrane bioreactor for municipal wastewater treatment. *Chem Eng Technol* **165**:175–183 (2010).
7 Katsoyiannis IA, Gkotsis P, Castellana M, Cartechini F and Zouboulis AI, Production of demineralized water for use in thermal power stations by advanced treatment of secondary wastewater effluent. *J Environ Manage* **190**:132–139 (2017).
8 Usman M, Zarebanadkouki M, Waseem M, Katsoyiannis IA and Ernst M, Mathematical modeling of arsenic(V) adsorption onto iron oxyhydroxides in an adsorption-submerged membrane hybrid system. *J Hazard Mater* **400**:123221 (2020). https://doi.org/10.1016/j.jhazmat.2020.123221.
9 Hu Y, Wang XC, Tian W, Ngo HH and Chen R, Towards stable operation of a dynamic membrane bioreactor (DMBR): operational process, behavior and retention effect of dynamic membrane. *J Membr Sci* **498**:20–29 (2016).
10 H-q C, D-w C, Jin W and Dong B-Z, Characteristics of bio-diatomite dynamic membrane process for municipal wastewater treatment. *J Membr Sci* **325**:271–276 (2008).
11 Aghili F, Ghoreyshi AA, Rahimpour A and Rahimnejad M, Coating of mixed-matrix membranes with powdered activated carbon for fouling control and treatment of dairy effluent. *Process Saf Environ* **107**:528–539 (2017).
12 Lu D, Cheng W, Zhang T, Lu X, Liu Q, Jiang J *et al*., Hydrophilic Fe_2O_3 dynamic membrane mitigating fouling of support ceramic membrane in ultrafiltration of oil/water emulsion. *Sep Purif Technol* **165**:1–9 (2016).
13 Tanny GB and Johnson JS, The structure of hydrous Zr(IV) oxide–polyacrylate membranes: poly(acrylic acid) deposition. *J Appl Polym Sci* **22**:289–297 (1978).
14 Cai Z and Benjamin MM, NOM fractionation and fouling of low-pressure membranes in microgranular adsorptive filtration. *Environ Sci Technol* **45**:8935–8940 (2011).
15 Huang H, Schwab K and Jacangelo JG, Pretreatment for low pressure membranes in water treatment: a review. *Environ Sci Technol* **43**:3011–3019 (2009).
16 Tian H, Sun L, Duan X, Chen X, Yu T, Feng C *et al*., Effect of phosphate on ultrafiltration membrane performance after predeposition of Fe_3O_4. *Environ Eng Sci* **35**:654–661 (2018).
17 Nyobe D, Ye J, Tang B, Bin L, Huang S, Fu F *et al*., Build-up of a continuous flow pre-coated dynamic membrane filter to treat diluted textile wastewater and identify its dynamic membrane fouling. *J Environ Manage* **252**:109647 (2019).
18 Noor MJMM, Ahmadun FR, Mohamed TA, Muyibi SA and Pescod MB, Performance of flexible membrane using kaolin dynamic membrane in treating domestic wastewater. *Desalination* **147**:263–268 (2002).
19 Wang JY, Chou KS and Lee CJ, Dead-end flow filtration of solid suspension in polymer fluid through an active kaolin dynamic membrane. *Sep Sci Technol* **33**:2513–2529 (1998).
20 O'Day PA, Vlassopoulos D, Meng X and Benning LG eds, *Advances in Arsenic Research*. ACS Symposium Series. American Chemical Society, Washington, DC (2005).
21 Smith AH, Hopenhayn-Rich C, Bates MN, Goeden HM, Hertz-Picciotto I, Duggan H *et al*., Cancer risks from arsenic in drinking water. *Environ Health Perspect* **97**:259–267 (1992).
22 Hindmarsh JT and McCurdy RF, Clinical and environmental aspects of arsenic toxicity. *Crit Rev Clin* **23**:315–347 (1986).
23 Podgorski J and Berg M, Global threat of arsenic in groundwater. *Science* **368**:845–850 (2020).
24 Pal BN, Granular ferric hydroxide for elimination of arsenic from drinking water. *Technologies for arsenic removal from drinking water*:59–68 (2001).
25 Wedepohl KH, Correns CW, Shaw DM, Turekian KK and Zemann J, *Handbook of Geochemistry*. Springer, Berlin (1969).
26 Ferguson JF and Gavis J, A review of the arsenic cycle in natural waters. *Water Res* **6**:1259–1274 (1972).

27 Masscheleyn PH, Delaune RD and Patrick WH, Effect of redox potential and pH on arsenic speciation and solubility in a contaminated soil. *Environ Sci Technol* **25**:1414–1419 (1991).
28 Alka S, Shahir S, Ibrahim N, Ndejiko MJ, Vo D-VN and Manan FA, Arsenic removal technologies and future trends: a mini review. *J Clean Prod* **278**:123805 (2021).
29 Mitrakas MG, Panteliadis PC, Keramidas VZ, Tzimou-Tsitouridou RD and Sikalidis CA, Predicting Fe^{3+} dose for As(V) removal at pHs and temperatures commonly encountered in natural waters. *Chem Eng J* **155**:716–721 (2009).
30 Zouboulis A and Katsoyiannis I, Removal of arsenate from contaminated water by coagulation-direct filtration. *Sep Sci Technol* **37**: 2859–2873 (2002).
31 Tubić A, Agbaba J, Dalmacija B, Ivancev-Tumbas I and Dalmacija M, Removal of arsenic and natural organic matter from groundwater using ferric and alum salts: a case study of central Banat region (Serbia). *J Environ Sci Health Part A* **45**:363–369 (2010).
32 Tripathy SS and Raichur AM, Enhanced adsorption capacity of activated alumina by impregnation with alum for removal of As(V) from water. *Chem Eng Technol* **138**:179–186 (2008).
33 Chwirka JD, Thomson BM and Stomp JM, Removing arsenic from groundwater. *J Am Water Works Assoc* **92**:79–88 (2000).
34 Wang L, Chen ASC, Sorg TJ and Fields KA, Field evaluation of As removal by IX and AA. *J Am Water Works Assoc* **94**:161–173 (2002).
35 Tresintsi S, Simeonidis K, Zouboulis A and Mitrakas M, Comparative study of As(V) removal by ferric coagulation and oxy-hydroxides adsorption: laboratory and full-scale case studies. *Desalin Water Treat* **51**:2872–2880 (2013).
36 Mohan D and Pittman CU, Arsenic removal from water/wastewater using adsorbents: a critical review. *J Hazard Mater* **142**:1–53 (2007).
37 Tresintsi S, Simeonidis K, Vourlias G, Stavropoulos G and Mitrakas M, Kilogram-scale synthesis of iron oxy-hydroxides with improved arsenic removal capacity: study of Fe(II) oxidation–precipitation parameters. *Water Res* **46**:5255–5267 (2012).
38 Amy GL, *Adsorbent Treatment Technologies for Arsenic Removal*. AWWA Research Foundation and American Water Works Association, Denver, CO (2005).
39 Ćurko J, Matošić M, Crnek V, Stulić V and Mijatović I, Adsorption characteristics of different adsorbents and Iron(III) salt for removing As (V) from water. *Food Technol Biotechnol* **54**:250–255 (2016).
40 Bretzler A, Nikiema J, Lalanne F, Hoffmann L, Biswakarma J, Siebenaller L *et al*., Arsenic removal with zero-valent iron filters in Burkina Faso: field and laboratory insights. *Sci Total Environ* **737**: 139466 (2020).
41 Khan SU, Farooqi IH, Usman M and Basheer F, Energy efficient rapid removal of arsenic in an electrocoagulation reactor with hybrid Fe/Al electrodes: process optimization using CCD and kinetic modeling. *Water* **12**:2876 (2020). https://doi.org/10.3390/w12102876.
42 Katsoyiannis IA, Mitrakas M and Zouboulis AI, Arsenic occurrence in Europe: emphasis in Greece and description of the applied full-scale treatment plants. *Desalin Water Treat* **54**:2100–2107 (2015).
43 Ghurye GL, Clifford DA and Tripp AR, Combined arsenic and nitrate removal by ion exchange. *J Am Water Works Assoc* **91**:85–96 (1999).
44 Sato Y, Kang M, Kamei T and Magara Y, Performance of nanofiltration for arsenic removal. *Water Res* **36**:3371–3377 (2002).
45 Kang M, Kawasaki M, Tamada S, Kamei T and Magara Y, Effect of pH on the removal of arsenic and antimony using reverse osmosis membranes. *Desalination* **131**:293–298 (2000).
46 Abejón A, Garea A and Irabien A, Arsenic removal from drinking water by reverse osmosis: minimization of costs and energy consumption. *Sep Purif Technol* **144**:46–53 (2015).
47 Víctor-Ortega MD and Ratnaweera HC, Double filtration as an effective system for removal of arsenate and arsenite from drinking water through reverse osmosis. *Process Saf Environ* **111**:399–408 (2017).
48 Wang L, Chen ASC, Sorg TJ and Supply W, *Costs of arsenic removal technologies for small water systems: US EPA arsenic removal technology demonstration program*. United States Environmental Protection Agency, Cincinnati, OH, p. 92 (2011).
49 Chen ASC, Sorg TJ and Wang L, Regeneration of iron-based adsorptive media used for removing arsenic from groundwater. *Water Res* **77**: 85–97 (2015).
50 Hering JG, Katsoyiannis IA, Theoduloz GA, Berg M and Hug SJ, Arsenic removal from drinking water: experiences with technologies and constraints in practice. *J Environ Eng* **143**:3117002 (2017).
51 Zhang J and Stanforth R, Slow adsorption reaction between arsenic species and goethite (α-FeOOH): diffusion or heterogeneous surface reaction control. *Langmuir* **21**:2895–2901 (2005).
52 Banerjee K, Amy GL, Prevost M, Nour S, Jekel M, Gallagher PM *et al*., Kinetic and thermodynamic aspects of adsorption of arsenic onto granular ferric hydroxide (GFH). *Water Res* **42**:3371–3378 (2008).
53 Sinha S, Lee N, Amy G, Innovative technologies for arsenic removal, in Water Quality and Treatment Conference, Seattle, WA (2002).
54 Usman M, Katsoyiannis I, Mitrakas M, Zouboulis A and Ernst M, Performance evaluation of small sized powdered ferric hydroxide as arsenic adsorbent. *Water* **10**:957 (2018). https://doi.org/10.3390/w10070957.
55 Driehaus W, Jekel M and Hildebrandt U, Granular ferric hydroxide: a new adsorbent for the removal of arsenic from natural water. *J Water Supply Res Technol* **47**:30–35 (1998).
56 Tresintsi S, Simeonidis K, Estradé S, Martinez-Boubeta C, Vourlias G, Pinakidou F *et al*., Tetravalent manganese feroxyhyte: a novel nanoadsorbent equally selective for As(III) and As(V) removal from drinking water. *Environ Sci Technol* **47**:9699–9705 (2013).
57 Usman M, Katsoyiannis I, Rodrigues JH and Ernst M, Arsenate removal from drinking water using by-products from conventional iron oxyhydroxides production as adsorbents coupled with submerged microfiltration unit. *Environ Sci Pollut Res* (2020). https://doi.org/10.1007/s11356-020-08327-w.
58 Sperlich A, Schimmelpfennig S, Baumgarten B, Genz A, Amy G, Worch E *et al*., Predicting anion breakthrough in granular ferric hydroxide (GFH) adsorption filters. *Water Res* **42**:2073–2082 (2008).
59 Kalaruban M, Loganathan P, Shim W, Kandasamy J and Vigneswaran S, Mathematical modelling of nitrate removal from water using a submerged membrane adsorption hybrid system with four adsorbents. *Appl Sci* **8**:194 (2018).
60 Piazzoli A and Antonelli M, Application of the homogeneous surface diffusion model for the prediction of the breakthrough in full-scale GAC filters fed on groundwater. *Process Saf Environ* **117**:286–295 (2018).
61 Dabizha A, Bahr C and Kersten M, Predicting breakthrough of vanadium in fixed-bed absorbent columns with complex groundwater chemistries: a multi-component granular ferric hydroxide–vanadate–arsenate–phosphate–silicic acid system. *Water Res X* **9**: 100061 (2020).
62 Zheng M, Xu C, Hu H, Ye Z and Chen X, A modified homogeneous surface diffusion model for the fixed-bed adsorption of 4,6-DMDBT on $Ag–CeO_x/TiO_2–SiO_2$. *RSC Adv* **6**:112899–112907 (2016).
63 Kim Y, Kim C, Choi I, Rengaraj S and Yi J, Arsenic removal using mesoporous alumina prepared via a templating method. *Environ Sci Technol* **38**:924–931 (2004).
64 Mantel T, Benne P, Parsin S and Ernst M, Electro-conductive composite gold–polyethersulfone–ultrafiltration–membrane: characterization of membrane and natural organic matter (NOM) filtration performance at different in-situ applied surface potentials. *Membranes* **8**: 64 (2018).
65 Crittenden JC, Trussell RR, Hand DW, Howe KJ and Tchobanoglous G, *MWH's Water Treatment: Principles and Design*. John Wiley & Sons, Third Edition, Hoboken, NJ (2012). https://doi.org/10.1002/9781118131473.
66 Worch E, *Adsorption Technology in Water Treatment: Fundamentals, Processes, and Modeling*. De Gruyter, Berlin (2012). https://doi.org/10.1515/9783110240238.
67 Derlon N, Grütter A, Brandenberger F, Sutter A, Kuhlicke U, Neu TR *et al*., The composition and compression of biofilms developed on ultrafiltration membranes determine hydraulic biofilm resistance. *Water Res* **102**:63–72 (2016).
68 Westerhoff P, Highfield D, Badruzzaman M and Yoon Y, Rapid small-scale column tests for arsenate removal in iron oxide packed bed columns. *J Environ Eng* **131**:262–271 (2005).
69 Cui J, Du J, Yu S, Jing C and Chan T, Groundwater arsenic removal using granular TiO_2: integrated laboratory and field study. *Environ Sci Pollut Res* **22**:8224–8234 (2015).

Journal of Chemical Technology and Biotechnology published by John Wiley & Sons Ltd on behalf of Society of Chemical Industry (SCI).